

## Effect of preparation methods on tosufloxacin tosylate/hydroxypropyl- $\beta$ -cyclodextrin inclusion complex

Jianfei Sun<sup>1,2</sup>, Hailong Hong<sup>1,2\*</sup>, Ning Zhu<sup>1,2</sup>, Limin Han<sup>1</sup>, Quanling Suo<sup>1</sup>

<sup>1</sup>College of Chemical Engineering, Inner Mongolia University of Technology, Hohhot 010051, China,

<sup>2</sup>Inner Mongolia Engineering Research Center for CO<sub>2</sub> Capture and Utilization, Hohhot 010051, China

The main purpose of this work was to compare the effects of the four preparation methods on the TFLX/HP- $\beta$ -CD inclusion complex. The effects of different preparation methods on the inclusion complex were investigated by SEM, DSC, PXRD, FT-IR and <sup>1</sup>H NMR. All the characterization information indicated that the four preparation methods could cause interaction between TFLX and HP- $\beta$ -CD, but the inclusion complex prepared by solvent evaporation has more reaction sites. Phase solubility experiments demonstrated that the inclusion reaction was spontaneous. In vitro dissolution experiments showed that the dissolution of the inclusion complex in water was: solvent evaporation method (64.39%) > grinding method (42.37%) > ultrasonic method (40.00%) > freezing method (36.08%), and all higher than pure TFLX and physical mixture. These results suggest that the solvent evaporation is the most suitable method for preparing TFLX/HP- $\beta$ -CD inclusion complexes.

**Keywords:** Tosufloxacin tosylate. Hydroxypropyl- $\beta$ -cyclodextrin. Methods. Inclusion complex.

### ABBREVIATIONS

TFLX, Tosufloxacin tosylate; HP- $\beta$ -CD, Hydroxypropyl- $\beta$ -cyclodextrin; CDs, Cyclodextrins; DMF, N, N-dimethylformamide; EE, Embedding efficiency; UV, UV-visible spectroscopy; SEM, Scanning electron microscopy; DSC, Differential scanning calorimetry; PXRD, Powder X-ray diffractometry; FT-IR, Fourier-transform infrared spectroscopy; <sup>1</sup>H NMR, Nuclear magnetic resonance; K, Stability constant;  $\Delta$ H, Enthalpy;  $\Delta$ G, Gibbs free energy;  $\Delta$ S, entropy; PM, Preparation of physical mixture; SM, Solvent evaporation method; GM, Grinding method; UM, Ultrasonic method; FM, Freeze-drying method;

### INTRODUCTION

Tosufloxacin tosylate (TFLX) is a third-generation quinolone antibacterial drug. It was originally developed by Toyama Chemical Co., Ltd. in 1986, followed by double-blind, comparative studies from 1987 to 1988, and was commercially available in 1990 (Niki, 2002). TFLX was approved for the treatment of respiratory infections, biliary tract infections, urinary tract infections and gastrointestinal infections. Subsequently, it was approved for additional indications including non-gonococcal urethritis, infectious diseases, plastic surgery, typhoid and paratyphoid fever (Niki, 2002; Yamaguchi, 2001) (see Figure 1A for the structural formula of TFLX). Compared with similar drugs (eg ofloxacin, ciprofloxacin, etc.), TFLX has been shown to have high antibacterial activity, especially against gram-positive bacteria, gram-negative bacteria, chlamydia, mycoplasma and anaerobes (Kohno, 2002; Deguchi *et al.*, 1993; Yoshida *et al.*, 1992). However, TFLX exhibits poor water solubility and low bioavailability during oral administration, which greatly limits its clinical application.

\*Correspondence: H. L. Hong. College of Chemical Engineering, Inner Mongolia University of Technology, Hohhot 010051, China. Phone: +86-471-6575722. Fax: +86-471-6575722. E-mail: honghailong\_1979@163.com (H. L. Hong). ORCID: <https://orcid.org/0000-0002-7533-4115>. Jianfei Sun: <https://orcid.org/0000-0001-8126-4988>. Ning Zhu: <https://orcid.org/0000-0002-7535-1310>

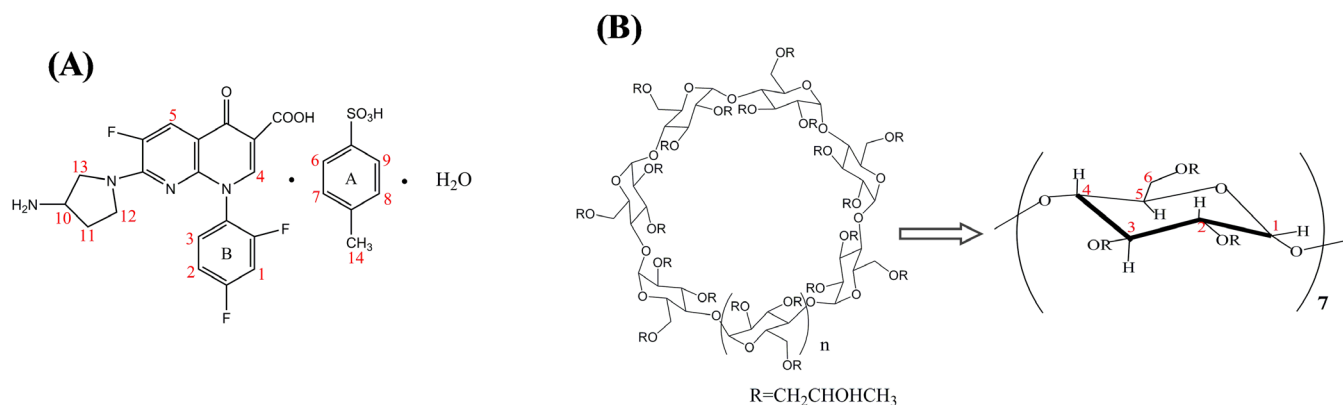


**FIGURE 1** - Structures of (A) TFLX and (B) HP-β-CD

Cyclodextrins (CDs) are a series of cyclic oligosaccharides formed by the hydrolysis and cyclization of starch by cyclodextrin glycosyltransferase (Tiwari *et al.*, 2010). Its structure consists of glucose units linked by α-1,4 glycosidic bonds of cyclic molecules, usually containing 6 to 12 D-glucopyranose units (Pereira *et al.*, 2007). The molecular morphology of CD is a conical cavity structure and has special properties of internal hydrophobicity and external hydrophilicity, in which the internal cavity can completely or partially wrap some guest molecules of suitable size and shape by means of hydrogen bonds or van der Waals forces (Li *et al.*, 2009). The most common CDs used as pharmaceutical excipients are α-, β- and γ-CDs containing six, seven and eight glucopyranose units, respectively (Li *et al.*, 2016). Hydroxypropyl-beta-cyclodextrin (HP-β-CD) is a derivative of β-CD (see Figure 1B for the structural formula of HP-β-CD) and clinical trials have shown that HP-β-CD is safe and tolerable in subjects without β-CD side effects (Li *et al.*, 2016; Pitha *et al.*, 1986). In addition, it has high water solubility and thermal stability and low toxicity. It has been confirmed that the solubility characteristics of HP-β-CD can be beneficial to increase the solubility of poorly soluble drugs and improve their bioavailability (Oh *et al.*, 1998; Ansari *et al.*, 2011).

In this study, the inclusion complexes of TFLX and HP-β-CD were prepared by solvent evaporation method, grinding method, ultrasonic method and freeze-drying method. Using the embedding efficiency as the evaluation index, the experiment was designed by L<sub>9</sub>(3<sup>4</sup>)

orthogonal table to determine the optimal inclusion process parameters. The effects of different methods on the formation of TFLX/HP-β-CD inclusion complexes were analyzed by SEM, DSC, XRD, FT-IR and <sup>1</sup>H NMR. The effect of different methods on the in vitro dissolution of TFLX/HP-β-CD inclusion complexes was studied using aqueous solution as the dissolution medium. Eventually, the best method for preparing TFLX and HP-β-CD inclusion complexes was determined.

## MATERIAL AND METHODS

### Material

TFLX was obtained from Chifeng Wanze Pharmaceutical Co., Ltd. (Chifeng China). HP-β-CD was obtained from Shandong Binzhou Zhiyuan Biotechnology Co., Ltd. (Binzhou, China). All chemical reagents and solvents used were of analytical grade and were purchased from Tianjin Fengchuan Chemical Reagent Technology Co., Ltd. (Tianjin, China). The solvent DMSO-d<sub>6</sub> was of spectroscopic NMR grade. Ultrapure water was used throughout the experiment.

### UV-visible spectroscopy (UV)

UV-visible spectrophotometer (UV-2450, Shimadzu, Japan) was first used to prove that HP-β-CD does not interfere with TFLX detection (Figure S1). Therefore, the TFLX content in the prepared inclusion complex was

analyzed by this method. TFLX (3.6 mg) was completely dissolved in DMF (50ml) in a volumetric flask, and the solution was diluted with DMF to various concentrations (2.88 μg/mL, 5.76 μg/mL, 11.52 μg/mL, 17.28 μg/mL, 23.04 μg/mL). The TFLX content in each solution was

determined by measuring the absorbance at 269 nm with UV-2450. As shown in Figure S2, a good linearity was observed in the range of 2-24 μg/ml. The concentration of TFLX was calibrated according to the calibration curve:  $y=0.0829x-0.0238$  ( $R^2=0.9994$ ).

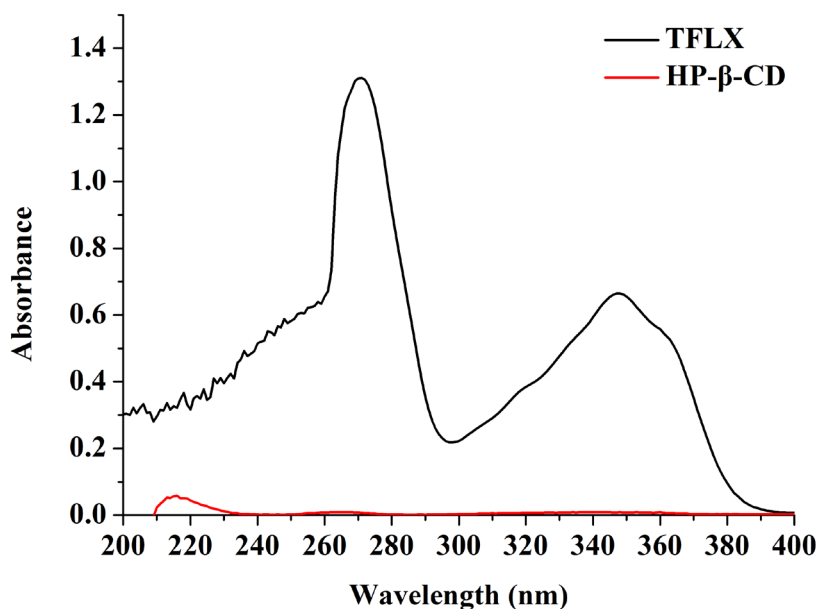


FIGURE S1 - The TFLX and HP-β-CD of UV absorption spectrum

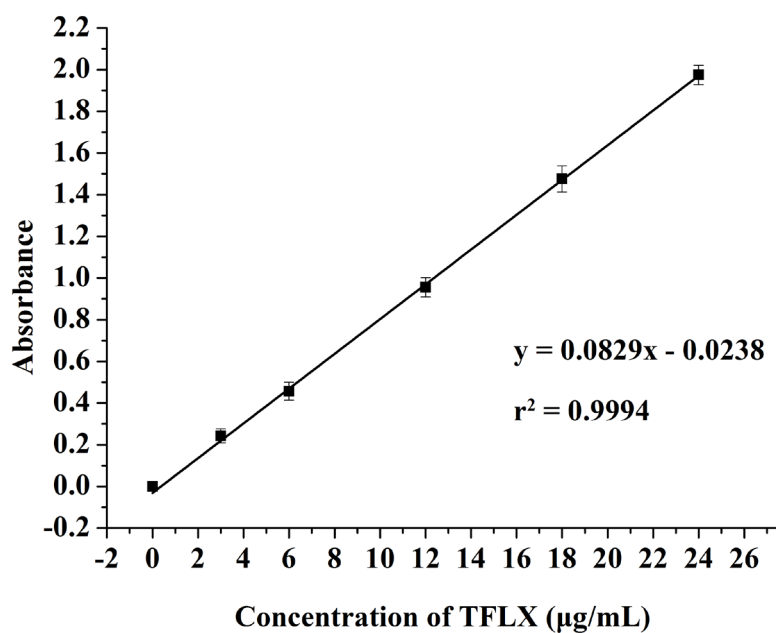


FIGURE S2 - Standard calibration curve of TFLX

## Embedding efficiency

The effects of temperature, molar ratio, inclusion time and power on the embedding efficiency (EE) were investigated. The embedding efficiency and drug loading can be calculated according to the following equations (1) and (2) (Wei *et al.*, 2017):

$$EE\% = \frac{\text{amount of TFLX entrapped}}{\text{initial TFLX amount}} \quad (1)$$

$$\text{Drug loading} = \frac{\text{amount of TFLX entrapped}}{\text{amount of inclusion complex}} \quad (2)$$

## Preparation of physical mixture (PM)

TFLX and HP- $\beta$ -CD were weighed in a 1:1 (0.2 g : 0.5185 g) molar ratio, placed in a beaker and stirred with a glass rod for 4 to 5 minutes until well mixed, and finally stored in a desiccator, which was TFLX and HP- $\beta$ -CD physical mixture, recorded as PM spare.

## Preparation of inclusion complexes

Inclusion complexes of TFLX and HP- $\beta$ -CD were prepared by solvent evaporation method, grinding method, ultrasonic method, freeze-drying method at a molar ratio of 1:1 (0.2 g : 0.5185 g), 1:2 (0.2 g : 1.0370 g) and 2:1 (0.4 g : 0.5185 g). The optimum preparation parameters were determined by orthogonal test. Orthogonal tests were used to determine the optimal process conditions (temperature, time, molar ratio, ultrasonic power, etc.) for different methods (SM, GM, UM, FM) of preparing inclusion complexes.

### Solvent evaporation method (SM)

As shown in Table SI, the optimum process condition is  $A_1B_2C_2D_1$ . 0.2 g TFLX was dissolved in 10 mL methanol, which was mixed with 0.5185 g HP- $\beta$ -CD in 10 mL of ultra-pure water. The mixed solution was placed on a magnetic stirrer and stirred at 100 r/min for 60 min. Subsequently, the mixed solution was evaporated under reduced pressure on a rotary evaporator at 50 °C, and vacuum dried to obtain TFLX/HP- $\beta$ -CD inclusion complex powder and stored for use (Ahn *et al.*, 2013).

**Table SI** - SM orthogonal test results table

Number	Factors				Embedding efficiency (%)
	A	B	C	D(Empty column)	
1	1 (1:1)	1 (40 °C)	1 (30 min)	1	52.40
2	1	2 (50 °C)	2 (60 min)	2	47.23
3	1	3 (60 °C)	3 (120 min)	3	33.78
4	2 (1:2)	1	2	3	47.14
5	2	2	3	1	50.44
6	2	3	1	2	27.52
7	3 (2:1)	1	3	2	28.74
8	3	2	1	3	35.45
9	3	3	2	1	42.08
$K_1$	133.41	128.28	115.37	144.92	$C_T=14784.94$
$K_2$	125.1	133.12	136.45	103.49	
$K_3$	106.27	103.38	112.96	116.37	
R	9.05	9.91	7.83	13.81	

**Grinding method (GM)**

As shown in Table SII, the optimum process condition is  $A_3B_1C_3D_2$ . 0.5785 g HP- $\beta$ -CD was added to a 1.5 mL ultrapure water mortar and ground uniformly, and then 0.4

g TFLX was added and ground together for 30 min. The mixture was frozen for 24 hours, and the free HP- $\beta$ -CD was washed away with a small amount of ultrapure water, vacuum-dried and ground to obtain a TFLX/HP- $\beta$ -CD inclusion complex powder (Xu *et al.*, 2015).

**Table SII** - GM orthogonal test results table

Number	Factors				Embedding efficiency (%)
	A	B	C	D(Empty column)	
1	1 (1:1)	1 (30 min)	1 (0.5 mL)	1	32.79
2	1	2 (1 h)	2 (1 mL)	2	58.98
3	1	3 (2 h)	3 (1.5 mL)	3	49.83
4	2 (1:2)	1	2	3	51.61
5	2	2	3	1	44.29
6	2	3	1	2	34.35
7	3 (2:1)	1	3	2	61.02
8	3	2	1	3	39.25
9	3	3	2	1	43.70
$K_1$	141.60	145.42	106.39	120.78	$C_T=19211.81$
$K_2$	130.25	142.52	154.29	154.35	
$K_3$	143.97	127.88	155.14	140.69	
R	13.72	17.54	48.75	33.57	

**Ultrasonic method (UM)**

As shown in Table SIII, the optimum process condition is  $A_1B_1C_1D_2$ . 0.2 g TFLX was dissolved in 10 mL methanol, 0.5185 g HP- $\beta$ -CD was dissolved in 10 mL of ultrapure water, and both solutions were mixed on a magnetic stirrer.

The mixed solution was sonicated in an ultrasonic oscillator at a temperature of 40 °C and an oscillation frequency of 150 W for 15 min. After that, it was frozen for 24 hours, suction filtered and the filter cake was washed with a small amount of ultrapure water, and vacuum dried to obtain a TFLX/HP- $\beta$ -CD inclusion complex (Tian *et al.*, 2013).

**Table SIII** - UM orthogonal test results table

Number	Factors				Embedding efficiency (%)
	A	B	C	D	
1	1 (1:1)	1 (40 °C)	1 (15 min)	1 (100 W)	66.77
2	1	2 (50 °C)	2 (30 min)	2 (150 W)	57.41
3	1	3 (60 °C)	3 (60 min)	3 (200 W)	46.76
4	2 (1:2)	1	2	3	12.98
5	2	2	3	1	16.03
6	2	3	1	2	30.36
7	3 (2:1)	1	3	2	23.22
8	3	2	1	3	20.71
9	3	3	2	1	18.45
K <sub>1</sub>	170.94	102.97	117.84	101.25	C <sub>T</sub> =9518.60
K <sub>2</sub>	59.37	94.15	88.84	119.99	
K <sub>3</sub>	62.38	95.57	86.01	89.45	
R	111.57	8.82	31.83	30.54	

### Freeze-drying method (FM)

As shown in Table SIV, the optimum process condition is A<sub>3</sub>B<sub>2</sub>C<sub>1</sub>D<sub>1</sub>. 0.4 g TFLX was dissolved in 10 mL methanol, 0.5185 g HP-β-CD was dissolved in 10 mL of ultrapure water. The TFLX solution was added

dropwise to the HP-β-CD solution, which was placed in a refrigerator at 2 °C and frozen for 6 h. Following filtration by suction, the filter cake was washed with a small amount of ultrapure water and vacuum dried to obtain the TFLX/HP-β-CD inclusion complex (Oguchi *et al.*, 1990).

**Table SIV** - FM orthogonal test results table

Number	Factors				Embedding efficiency (%)
	A	B	C	D(Empty column)	
1	1 (1:1)	1 (0 °C)	1 (6 h)	1	13.68
2	1	2 (2 °C)	2 (12 h)	2	16.50
3	1	3 (4 °C)	3 (18 h)	3	15.53
4	2 (1:2)	1	2	3	11.09
5	2	2	3	1	19.38
6	2	3	1	2	18.25
7	3 (2:1)	1	3	2	33.50
8	3	2	1	3	42.90
9	3	3	2	1	41.99
K <sub>1</sub>	45.71	58.27	74.83	75.05	C <sub>T</sub> =6258.03
K <sub>2</sub>	48.72	78.78	69.58	68.25	
K <sub>3</sub>	118.39	75.77	68.41	68.61	
R	72.68	20.51	6.42	6.8	

### Phase solubility studies of TFLX in HP- $\beta$ -CD

Phase solubility studies were performed according to the procedure described (Higuchi *et al.*, 1965). Excess TFLX (0.74 g) was added to an aqueous solution containing different concentrations of HP- $\beta$ -CD (0, 2, 4, 8, 12, 16, 20 mM). The suspension was shaken at 30 °C for 24 h until the solubility reached equilibrium, then the sample was passed through a 0.22  $\mu$ m membrane filter to remove excess TFLX. The absorbance of TFLX in the filtrate was determined by UV-2450 and the concentration of TFLX was calculated by the standard curve (Figure S2). The purpose was to reflect the reproducibility of the data, the phase solubility at 40 °C, 50 °C and 60 °C were measured with the same method. The solubility diagrams at different temperatures were all classified as the A<sub>L</sub> type of Higuchi, which proved that the inclusion reaction was feasible. Since the maximum stability constant was obtained at 50 °C, the phase solubility studies at different pH conditions were chosen at this temperature. Next, according to the Chinese Pharmacopoeia, and at 50 °C, the similar phase solubility study was also performed

on behalf of the gastrointestinal tract pH 1.2 (hydrochloric acid buffer), 4.5 (acetic acid-sodium acetate buffer), 6.8 (phosphate buffer), 7.4 (phosphate buffer), and the concentration of HP- $\beta$ -CD was selected to be 0, 2, 4, 8, 12 mM. The stability constant can be calculated from the slope of the fitted curve of the phase solubility diagram, equation (3) (Soares *et al.*, 2009):

$$K = \frac{\text{slope}}{S_0(1 - \text{slope})} \quad (3)$$

where  $S_0$  is the solubility of TFLX in the absence of HP- $\beta$ -CD.

The enthalpy of complexation ( $\Delta H$ ) was determined using the Van't Hoff equation (Equation (4)). The Gibbs free energy ( $\Delta G$ ) and entropy ( $\Delta S$ ) at the time of complexation were determined using equations (5) and (6) (Wei *et al.*, 2017).

$$\ln \frac{K_2}{K_1} = \Delta H \frac{(T_2 - T_1)}{RT_2T_1} \quad (4)$$

$$\Delta G = -RT \ln K \quad (5)$$

$$\Delta S = \frac{(\Delta H - \Delta G)}{T} \quad (6)$$

### Dissolution studies

The dissolution of the sample in ultrapure water was investigated using an RCZ-8M dissolution tester (TDTF Technology Co., Ltd., China) ( $37 \pm 0.5$  °C,  $V=1000$  mL) with paddle speed of 100 rpm. Accurately weigh 5 mg of TFLX and the equivalent of 5 mg of the physical mixture and inclusion complex in the weighing paper, and then simultaneously added to the dissolution cup containing 1000 mL of solvent. Each sample solution (10 mL) was extracted at 2, 5, 8, 11, 15, 20, 30, 40, 55, 75, and 105 minutes intervals through a  $0.45 \mu\text{m}$  millipore filter. The samples were analyzed at 269 nm with UV-2450 and the concentration of TFLX was calculated according to the standard calibration curve (Figure S2) as described above (Jun *et al.*, 2007). All experiments were performed in triplicate.

### Characterization of inclusion complexes

In order to investigate the correlation between TFLX and HP- $\beta$ -CD, the inclusion complex was characterized using differential scanning calorimetry (DSC), powder X-ray diffraction (PXRD), scanning electron microscopy (SEM), fourier transform infrared spectroscopy (FT-IR) and nuclear magnetic resonance ( $^1\text{H}$  NMR). Through the comparative analysis of various characterization means, the effects of different preparation methods on inclusion complexes were studied.

### Differential scanning calorimetry (DSC)

The samples were performed in the STA 449F3 DSC system (NETZSCH, Germany) using a dynamic atmosphere of nitrogen. Each sample (5 mg) was heated from 25 °C to 1000 °C at 10 °C/min with an empty alumina crucible as a reference.

### Scanning electron microscopy (SEM)

The surface morphology of TFLX, HP- $\beta$ -CD, physical mixture, inclusion complex was obtained by scanning electron microscopy (HITACHI-SU8220, Japan). Each sample was manually dispersed in the conductive adhesive attached to the aluminum sheet.

### Powder X-ray diffractometry (PXRD)

Powder X-ray diffraction patterns of the samples were obtained using a X-ray diffractometer (XRD-6000, Shimadzu, Japan) with Cu  $K\alpha$  radiation. The used current was 30 mA and the voltage was 40 kV. The sample measured diffraction angle  $2\theta$  in the range of 5-80°, scanning speed of 1.5 °/min and step size of 0.05°.

### Fourier-transform infrared spectroscopy (FT-IR)

FT-IR spectra of TFLX, HP- $\beta$ -CD, physical mixtures, TFLX/HP- $\beta$ -CD inclusion complexes were measured in a scanning range of 4000-400  $\text{cm}^{-1}$  using a FT-IR spectrometer (PerkinElmer Spectrum Two, USA). Each sample was applied to a spectrometer after KBr tableting.

### $^1\text{H}$ NMR spectroscopy ( $^1\text{H}$ NMR)

The  $^1\text{H}$  NMR spectra of TFLX, HP- $\beta$ -CD, physical mixtures and the four inclusion complexes were obtained with an INOVA 500 MHz NMR Spectrometer (Varian, USA). All samples were dissolved in DMSO- $d_6$  and their  $^1\text{H}$  NMR spectra were determined.

## RESULTS AND DISCUSSION

### Scanning electron microscopy (SEM)

The SEM images of TFLX, HP- $\beta$ -CD, the physical mixture, the TFLX/HP- $\beta$ -CD inclusion complex prepared by SM, GM, UM, FM are showed in Figure 2. TFLX was presented in various sizes of block structures (Figure 2a), while HP- $\beta$ -CD appeared as spherical particles with a cavity structure (Figure 2b). The cavity structure of HP- $\beta$ -CD and the block structure of TFLX were observed in

the SEM of the physical mixture (Figure 2c), indicating that the two components were simply mixed. The SEM images of TFLX/HP- $\beta$ -CD inclusion complexes prepared by SM revealed large particles in the solid state (Figure 2d), indicating that complexes were formed between TFLX and HP- $\beta$ -CD. The SEM images of the TFLX/HP- $\beta$ -CD inclusion complexes prepared by UM and FM were very similar (Figure 2e and 2g) and all exhibited

a homogeneous rod-like structure, and the morphology of TFLX and HP- $\beta$ -CD disappeared, demonstrating the formation of TFLX/HP- $\beta$ -CD inclusion complexes. From the SEM images of TFLX/HP- $\beta$ -CD inclusion complexes prepared by GM (Figure 2f), the block structure of TFLX was observed, but the HP- $\beta$ -CD morphology disappeared. This may be due to only a partial interaction between the two and the presence of free TFLX.

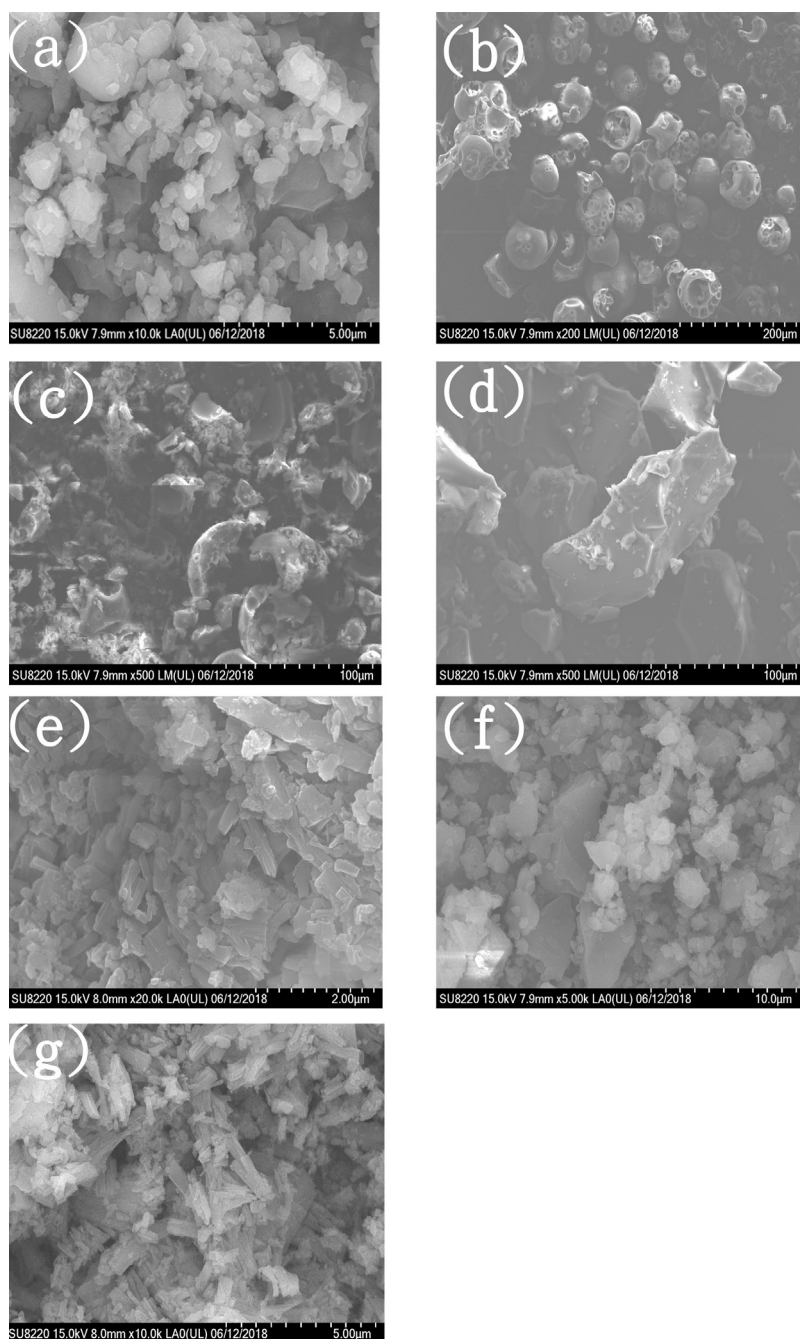


**FIGURE 2** - SEM images of (a) TFLX, (b) HP- $\beta$ -CD, (c) physical mixture, inclusion complexes by (d) SM, (e) UM, (f) GM, (g) FM

### Differential scanning calorimetry (DSC)

The DSC thermograms of TFLX, HP- $\beta$ -CD, the physical mixture, the prepared TFLX/HP- $\beta$ -CD inclusion complexes by SM, GM, UM, FM are showed in Figure 3. The DSC curve of TFLX exhibited a obvious endothermic melting peak at 252 °C, and two wide exothermic peaks appeared at 380 °C and 937 °C. No characteristic endothermic peak was observed on the DSC curve of HP- $\beta$ -CD, but there was a broad exothermic peak at 373-390 °C. The DSC curve of the physical mixture exhibited a sharp endothermic peak at about 237 °C, probably because the mixture had a lower melting point than TFLX alone. However, no characteristic endothermic peaks of TFLX were observed in the inclusion complexes

prepared by SM, UM, GM, FM at 937 °C, indicating that the exothermic peak may be covered by HP- $\beta$ -CD. By comparing the DSC curves, the endothermic melting point peak of the inclusion complex prepared by FM was close to the physical mixture, indicating that TFLX was combined with HP- $\beta$ -CD with weaker interaction forces. The inclusion complexes prepared by SM and GM have lower endothermic peaks than TFLX, but SM was relatively lower, indicating that this method was more likely to combine drugs to form an inclusion complex. The endothermic peak of the inclusion complex prepared by UM was also close to the physical mixture, and the exothermic peak of TFLX was present, indicating that the method was not suitable for the preparation of the TFLX/HP- $\beta$ -CD inclusion complex.

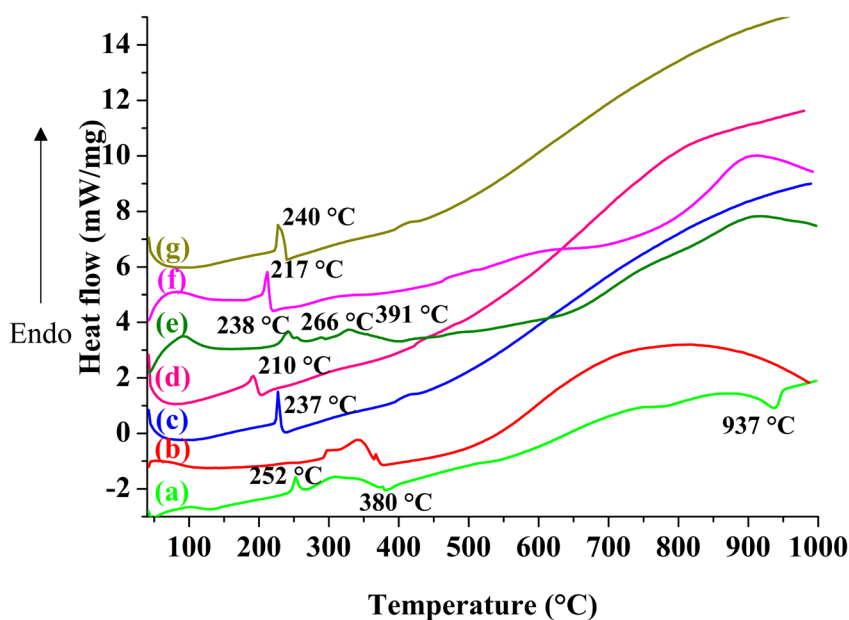


**FIGURE 3** - DSC curves of TFLX, physical mixture and inclusion complexes by SM, UM, GM, FM

### Powder X-ray diffractometry (PXRD)

The PXRD spectra of TFLX, HP- $\beta$ -CD, the physical mixture, the TFLX-HP- $\beta$ -CD inclusion complexes prepared by SM, GM, UM, FM are shown in Figure 4. The diffractogram of TFLX was exhibited with many characteristic peaks at diffraction angles ( $2\theta$ ) of 5.0, 10.6, 10.7, 13.3, 15.3, 15.8, 18.6, 19.9, 20.5, 21.3, 22.4, 23.2,

26.0 and 30.0 (Figure 4a). This result revealed that TFLX exists in a crystalline state. In contrast, HP- $\beta$ -CD (Figure 4b) was present in an amorphous form due to the lack of characteristic crystallization peaks. From the shape of the obtained physical mixture (Figure 4c), it was found to be a superposition of the pattern of TFLX and HP- $\beta$ -CD. Compared to the diffraction patterns of TFLX and HP- $\beta$ -CD, the diffraction pattern of the inclusion complex

prepared by SM (Figure 4d) was comparable to amorphous HP- $\beta$ -CD, and the apparent crystallization peak of TFLX disappears, which may be attributed to the TFLX molecule was encapsulated in the cavity of HP- $\beta$ -CD. From Figure 4e, the inclusion complex prepared by UM showed a new peak at a diffraction angle of 6.6, and the characteristic peak at the diffraction angle of 19.9, 20.5, 26.0 disappeared, indicating that some interaction may occur between TFLX and HP- $\beta$ -CD. Only the weakening of the characteristic

peak was observed in the inclusion complex prepared by GM (Figure 4f), suggesting that the two components may interact but the force was not strong. The inclusion complex prepared by FM (Figure 4g) showed a new peak at a diffraction angle of 6.6, and other characteristic peaks were significantly weakened, demonstrating some interactions between the two components. The above results indicate that the preparation process by SM was most likely to form inclusion complexes.

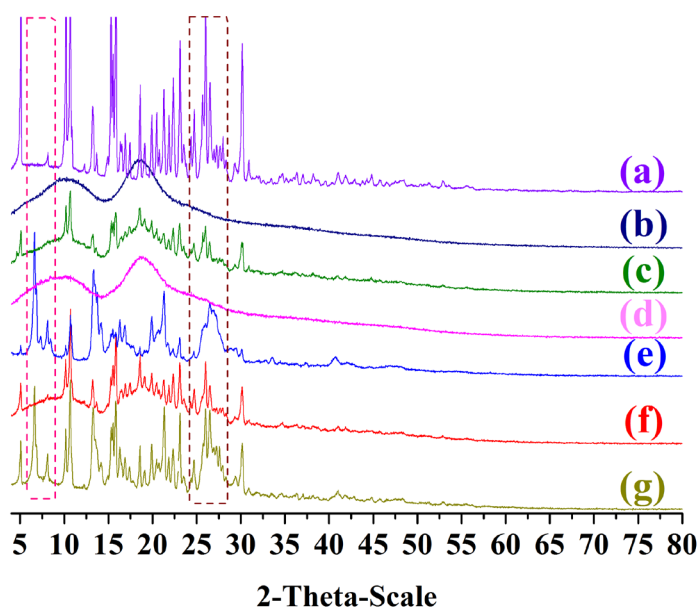


**FIGURE 4** - Powder X-ray diffractogram (a) TFLX, (b) HP- $\beta$ -CD, (c) physical mixture, inclusion complexes by (d) SM, (e) UM, (f) GM, (g) FM

### FT-IR spectroscopy (FT-IR)

The FTIR spectra of TFLX, HP- $\beta$ -CD, the physical mixture, the prepared TFLX/HP- $\beta$ -CD inclusion complexes by SM, GM, UM, FM are displayed in Figure 5. The FT-IR spectrum of TFLX shows strong absorption bands at 3435  $\text{cm}^{-1}$ , 3067-2964  $\text{cm}^{-1}$ , 1736  $\text{cm}^{-1}$ , 1634  $\text{cm}^{-1}$ , 1501  $\text{cm}^{-1}$ , 1448  $\text{cm}^{-1}$ , 1378-1365  $\text{cm}^{-1}$ , 1277  $\text{cm}^{-1}$ , 1172-1035  $\text{cm}^{-1}$ , 856-508  $\text{cm}^{-1}$  (Figure 5a). The FT-IR spectrum of HP- $\beta$ -CD exhibits prominent absorption bands at 3355  $\text{cm}^{-1}$ , 2917  $\text{cm}^{-1}$ , 1021  $\text{cm}^{-1}$  (Figure 5b). The free stretching vibration of OH was represented at 3355  $\text{cm}^{-1}$ . The stretching vibrations of  $\text{CH}_3$  and CH were

shown at 2917  $\text{cm}^{-1}$ . The large absorption band at 1021  $\text{cm}^{-1}$  corresponds to the stretching vibration of C-O-C. In the FT-IR spectra of the physical mixture (Figure 5c), the characteristic peaks of both TFLX and HP- $\beta$ -CD were observed, indicating weaker associations between host and guest molecules. In the FT-IR spectrum of inclusion complexes prepared by SM (Figure 5d), disappearance or weakening of peaks occurred at 3067  $\text{cm}^{-1}$  ( $\nu_{\text{C}=\text{C}}$  on the benzene ring), 2924  $\text{cm}^{-1}$  ( $\nu_{\text{CH}}$ ), 1736  $\text{cm}^{-1}$  ( $\nu_{\text{C}=\text{O}}$ ), 1634  $\text{cm}^{-1}$  ( $\nu_{\text{C}=\text{C}}$ ), 1501  $\text{cm}^{-1}$  ( $\nu_{\text{C}=\text{C}}$ ), 1365  $\text{cm}^{-1}$  ( $\nu_{\text{CH}}$ ), 1227  $\text{cm}^{-1}$  ( $\nu_{\text{C}-\text{N}}$ ), 1172  $\text{cm}^{-1}$  ( $\nu_{\text{C}-\text{N}}$ ), 1108  $\text{cm}^{-1}$  ( $\delta_{\text{NH}}$ ), 1035  $\text{cm}^{-1}$  ( $\nu_{\text{C}-\text{F}}$ ), 856  $\text{cm}^{-1}$  ( $\delta_{\text{CH}}$ , adjacent hydrogen on the benzene ring), indicating that the peaks of these regions

were covered by HP- $\beta$ -CD. In the FT-IR spectrum of the inclusion complex prepared by UM (Figure 5e), the peak disappeared at 1501  $\text{cm}^{-1}$ , 1172  $\text{cm}^{-1}$ , and the peak intensity at 1108  $\text{cm}^{-1}$ , 1035  $\text{cm}^{-1}$  weakened. In the FT-IR spectrum of the inclusion complex prepared by GM (Figure 5f), the peak disappeared at 856  $\text{cm}^{-1}$ . However,

the spectrum of the inclusion complex prepared by FM (Figure 5g) was similar to that of TFLX, which only showed a decrease in the intensity of the characteristic peaks. By comparison, it was found that there are many sites of interaction between TFLX and HP- $\beta$ -CD in inclusion complexes prepared by

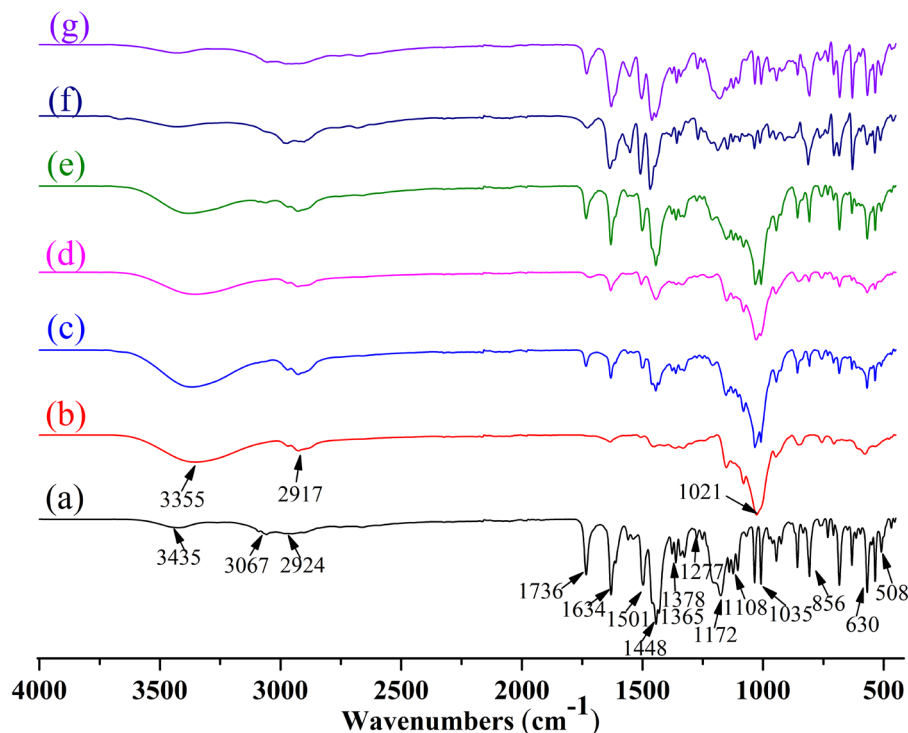


**FIGURE 5** - FT-IR spectra of (a) TFLX, (b) HP- $\beta$ -CD, (c) physical mixture, inclusion complexes by (d) SM, (e) UM, (f) GM, (g) FM

### NMR spectroscopy ( $^1\text{H}$ NMR)

$^1\text{H}$  NMR spectroscopy is commonly used to obtain the chemical shift values of host and guest molecules and provide evidence for the formation of inclusion complexes in solution (Tian *et al.*, 2013). The chemical shift change was calculated by the equation: where  $\Delta\delta = \delta(\text{complex}) - \delta(\text{free})$ . As shown in Figure 6a, the TFLX spectra of  $^1\text{H}$  (500 MHz, DMSO- $d_6$ , TMS) were  $\delta$  ppm: 7.560-7.615 (m, 1H, H-1), 7.336-7.370 (td, 1H, H-2), 7.786-7.833 (m, 1H, J=7.81 Hz, H-3), 8.836 (s, 1H, H-4), 8.101-8.126 (d, 1H, J=12.5 Hz, H-5), 7.462-7.478 (d, 2H, H-6, 9), 7.093-7.109 (d, 2H, H-7, 8), 2.637 (m, 1H, H-12), 2.275 (s, 3H, H-14), 7.999 (brs, 2H,  $\text{NH}_2$ ), 3.871 (brs, 4H, H-11, 13), 2.205 (m,

2H, H-10). As shown in Figure 6b, the HP- $\beta$ -CD spectra of  $^1\text{H}$  (500 MHz, DMSO- $d_6$ , TMS) were  $\delta$  ppm: 5.027 (H-1), 3.622 (H-2), 3.757 (H-3), 3.315 (H-4), 3.569 (H-5), 3.486 (H-6), 1.032 ( $\text{CH}_2$ ).

The  $^1\text{H}$  spectral chemical shift values of HP- $\beta$ -CD in inclusion complexes prepared by SM and GM were similar:  $\Delta\delta$  (-0.009, H-3), from which it was concluded that the drug enters the internal cavity of HP- $\beta$ -CD from the wide side. The  $^1\text{H}$  spectral chemical shift value of TFLX in the inclusion complex prepared by SM (Figure 6c) was relatively large:  $\Delta\delta$  (-0.021, H-1),  $\Delta\delta$  (-0.006, H-2),  $\Delta\delta$  (0.026, H-5),  $\Delta\delta$  (0.019, H-7, 8),  $\Delta\delta$  (-0.007, H-14), H-11, 13 disappears and active hydrogen on  $\text{NH}_2$  disappears. The  $^1\text{H}$  spectra of the

inclusion complexes prepared by GM (Figure 6d) and the complexes prepared by SM were similar, but there was an  $\text{NH}_2$  peak ( $\Delta \delta -0.075$ , 2H) in the inclusion complexes prepared by GM. The inclusion complexes prepared by UM (Figure 6e) and FM (Figure 6f) had no peak of HP- $\beta$ -CD, and there was no  $\text{NH}_2$  peak compared with the  $^1\text{H}$  spectrum of TFLX.

These results indicate that HP- $\beta$ -CD interacts more readily with TFLX in the inclusion complexes prepared by SM and GM, and suggest that the phenyl group (A ring, B ring), pyrrolidine and naphthyridine ring protons of TFLX deeply penetrated into the cavity of HP- $\beta$ -CD. However, inclusion complexes prepared by UM and FM do not demonstrate that TFLX enters the cavity of HP- $\beta$ -CD.

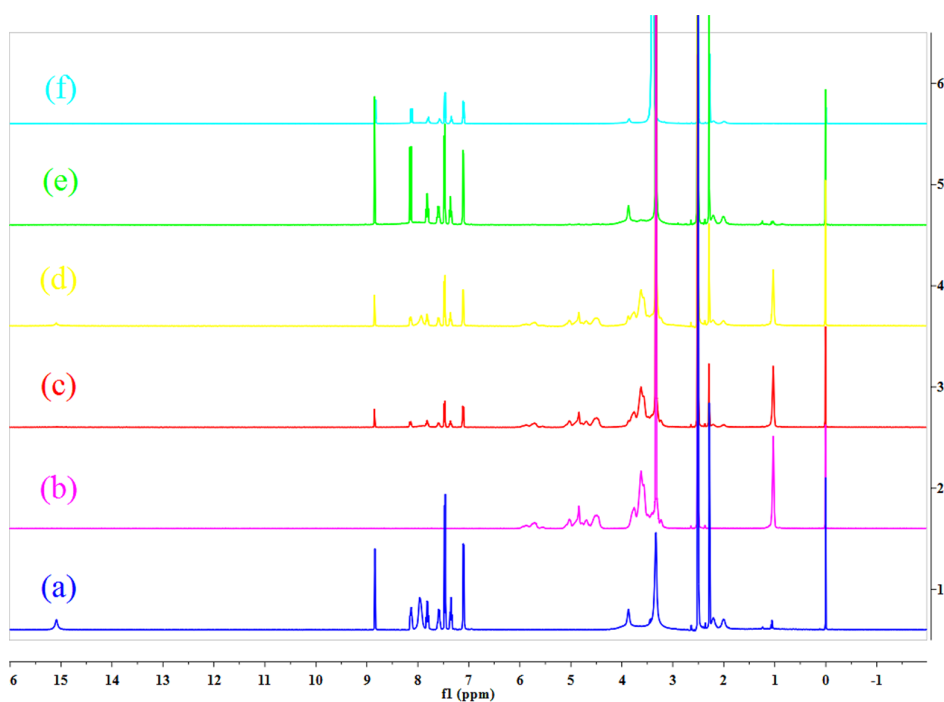


**FIGURE 6** -  $^1\text{H}$  NMR spectra of (a) TFLX, (b) HP- $\beta$ -CD, inclusion complexes by (c) SM, (d) UM, (e) GM, (f) FM

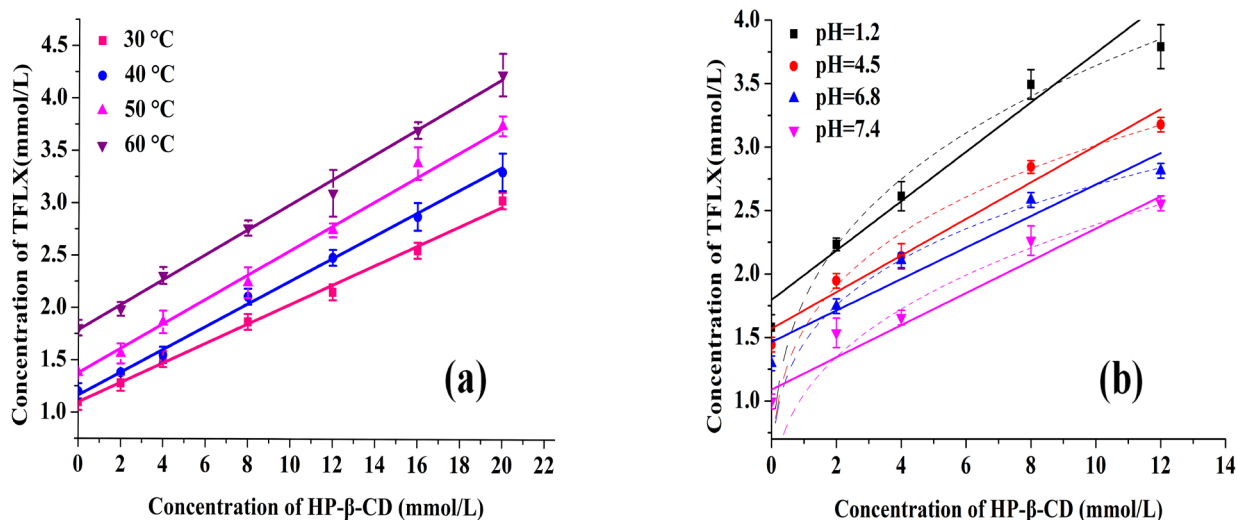
### Phase solubility studies

A linear correlation between the water solubility of TFLX and the concentration of HP- $\beta$ -CD solution was observed in the phase solubility diagram at 30, 40, 45 and 50  $^{\circ}\text{C}$ . According to Higuchi and Connors (1965) classification, the phase solubility curve is linear  $A_L$  type. The stability constant ( $K$ ) and the thermodynamic parameters ( $\Delta H$ ), ( $\Delta G$ ), ( $\Delta S$ ) of the complex were listed in Table SV. It can be seen from Figure 7a, at the same concentration of HP- $\beta$ -CD, the concentration of TFLX changes with increasing temperature, revealing that

temperature has a certain effect on the complexation reaction. However, Figure 7b shows that at different pH conditions, as the concentration of HP- $\beta$ -CD increased, the concentration of TFLX increased first, and then the increase trend slows down. Also, as the pH increased from 1.2 to 7.4, the concentration of TFLX decreased. Additionally, the  $\Delta G$  was negative, indicating that the complexation between TFLX and HP- $\beta$ -CD was spontaneous. The  $\Delta H$  and  $\Delta S$  were positive values, suggesting that the complexation reaction was an endothermic process and the encapsulation process was thought to be caused by entropy driving (Wei *et al.*, 2017).

**Table SV** - Thermodynamic parameters of inclusion complexes at different temperatures

T (°C)	Equations	R <sup>2</sup>	K (L/mol)	ΔG (KJ/mol)	ΔH (KJ/mol)	ΔS (J/mol*K)
30	Y=0.0936X+1.0141	0.9960	101.83	-10.27		
40	Y=0.1055X+1.1324	0.9916	104.15	-12.10		
50	Y=0.1305X+1.2367	0.9815	121.36	-12.89	7.32	60.15
60	Y=0.1148X+1.7057	0.9856	76.03	-12.00		

**FIGURE 7** - Phase solubility diagram of (a) TFLX/HP-β-CD system at different temperatures; (b) TFLX/HP-β-CD system at different pH conditions

### Dissolution study

Dissolution studies were used to evaluate the increase in dissolution rate of TFLX, physical mixture and inclusion complexes in ultrapure water as dissolution media. The cumulative dissolution percentage of the TFLX after 90 minutes was less than 13.99%, while the value of the physical mixture reached 20.74% after

100 minutes. The cumulative dissolution percentage of the inclusion complex prepared by SM, GM, UM, FM was 64.39%, 42.37%, 40.00%, and 36.08%, respectively (Figure 8). Obviously, the dissolution profiles of all inclusion complexes were higher than TFLX and physical mixtures, and the dissolution of the inclusion complexes prepared by SM was approximately 4.6 times that of pure TFLX.

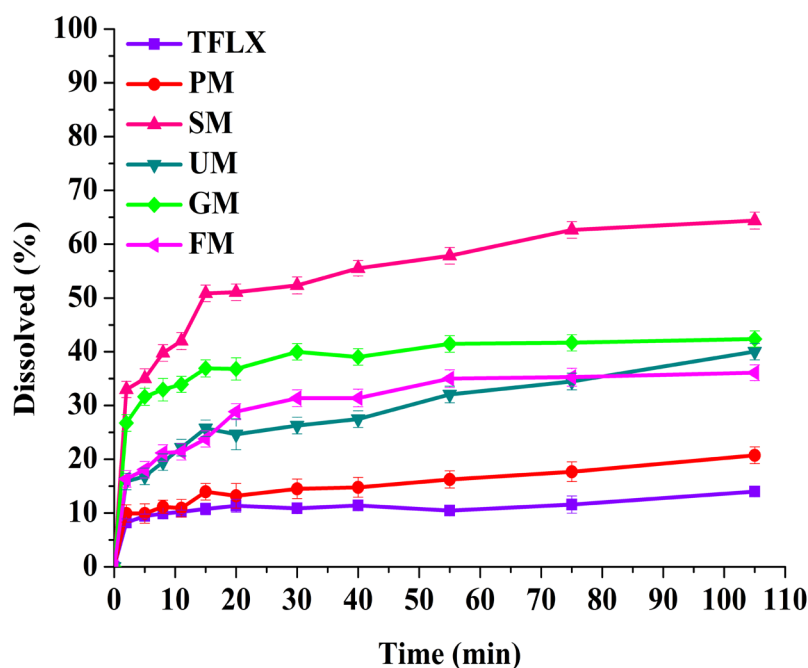


**FIGURE 8** - Dissolution profiles of TFLX, physical mixture and inclusion complexes by SM, UM, GM, FM

## CONCLUSIONS

In our present study, the inclusion complex TFLX/HP- $\beta$ -CD was efficiently prepared and characterized and its in vitro dissolution was determined. The SEM results revealed that the inclusion complex prepared by SM exhibited large particles, and both UM and FM exhibited a homogeneous rod-like structure, and GM could observe the morphology of part of TFLX, but these information all confirmed the formation of inclusion complex. DSC curves displayed that the inclusion complex prepared by SM had a lower endothermic melting point peak, followed by GM, whereas the melting peaks of the inclusion complex prepared by UM and FM were close to the physical mixture. The PXRD spectrum demonstrated that the inclusion complex prepared by SM was in an amorphous state, while the inclusion complex prepared by UM, GM, and FM only showed the disappearance or production of characteristic peaks, indicating that the inclusion reaction by the SM process was more thorough. FT-IR combined with  $^1\text{H}$  NMR spectroscopy showed that the interaction between TFLX and HP- $\beta$ -CD in the inclusion complex prepared by SM, GM was phenyl group (A ring, B ring), pyrrolidine and naphthyridine ring

protons, which enter the internal cavity of HP- $\beta$ -CD from the wide side, but the inclusion complex prepared by UM and FM does not prove that the proton of TFLX enters the cavity of HP- $\beta$ -CD. The results of in vitro dissolution showed that the inclusion complex prepared by SM had a dissolution rate of 64.39% in ultrapure water, about 4.6 times that of pure TFLX, followed by GM, which may have a certain solubilization effect with its smaller particle size. Therefore, our research indicates that SM is the best method for preparing TFLX/HP- $\beta$ -CD inclusion complex.

## DECLARATIONS

### Acknowledgements

The authors are very grateful to the National Natural Science Foundation of China (Grant No. 21666026) and the Natural Science Foundation of Inner Mongolia (Grant No. 2015MS0204) for their financial support in the experimental work.

## CONFLICT OF INTEREST

No conflict of interest associated with this work.

## REFERENCES

- Ansari MT, Batty KT, Iqbal I, Sunderland VB. Improving the solubility and bioavailability of dihydroartemisinin by solid dispersions and inclusion complexes. *Arch Pharm Res*. 2011,34(5): 757-765.
- Ahn BK, Sang GL, Kim SR, Lee DH, Oh MH. Inclusion compound formulation of hirsutenone with beta-cyclodextrin. *J Pharm Invest*. 2013,43(6): 453-459.
- Deguchi T, Kawada Y, Saito I, Okazaki T. Clinical study of tosufloxacin tosylate in the treatment of non-gonococcal urethritis. *Jpn J Chemother*. 1993,41(3): 376-391.
- Higuchi T, Connors, KA. Phase solubility technique. *Adv Anal Chem Instrum*. 1965,4: 117-212.
- Jun SW, Kim MS, Kim JS, Park HJ, Lee S, Woo JS, Hwang SJ. Preparation and characterization of simvastatin/hydroxypropyl- $\beta$ -cyclodextrin inclusion complex using supercritical antisolvent (SAS) process. *Eur J Pharm Biopharm*. 2007,66(3): 413-421.
- Kohno S. Clinical assessment of tosufloxacin tosylate. *J Infect Chemother*. 2002,8(1): 19-27.
- Li J, Zhang M, Chao J, Shuang S. Preparation and characterization of the inclusion complex of Baicalin (BG) with beta-CD and HP-beta-CD in solution: an antioxidant ability study. *Spectrochimica Acta Part A*. 2009,73(4): 752-756.
- Li Y, Li F, Cai H, Chen X, Sun W. Structural characterization of inclusion complex of arbutin and hydroxypropyl- $\beta$ -cyclodextrin. *Trop J Pharm Res* Octoer, 2016,15(10): 2227-2233.
- Niki Y. Pharmacokinetics and safety assessment of tosufloxacin tosylate. *J Infect Chemother*. 2002,8(1): 1-18.
- Oh I, Lee MY, Lee YB, Shin SC, Park I. Spectroscopic characterization of ibuprofen/2-hydroxypropyl- $\beta$ -cyclodextrin inclusion complex. *Int J Pharmaceut*. 1998,175(2): 215-223.
- Oguchi T, Okada M, Yonemochi E, Yamamoto K, Nakaiet Y. Freeze-drying of drug-additive binary systems III. Crystallization of  $\alpha$ -cyclodextrin inclusion complex in freezing process. *Int J Pharm*. 1990,61(1): 27-34.
- Pereira, Moura CS, Defreitas AF, Freitas LCG, Lins RD. Revisiting the internal conformational dynamics and solvation properties of cyclodextrins. *J Braz Chem Soc*. 2007,18(18): 951-961.
- Pitha J, Milecki J, Fales H, Pannell L. Hydroxypropyl- $\beta$ -cyclodextrin: preparation and characterization; effects on solubility of drugs. *Int J Pharm*. 1986,29(1): 73-82.
- Soares LA, Ana Flávia Vasconcelos Borges Leal, Fraceto LF, Maia ER, Resck IS, Kato JM, Eric de Sousa Gil, Aparecido Ribeiro de Sousa, Luiz Carlos da Cunha, Kênnia Rocha Rezende. Host-guest system of 4-nerolidylcatechol in 2-hydroxypropyl- $\beta$ -cyclodextrin: preparation, characterization and molecular modeling. *J Incl Phenom Macrocycl Chem*. 2009,64(1-2): 23-35.
- Tian Y, Zhu Y, Bashari M, Hu X, Xu X. Identification and releasing characteristics of high-amylose corn starch-cinnamaldehyde inclusion complex prepared using ultrasound treatment. *Carbohydr Polym*. 2013,91(2): 586-589.
- Tiwari G, Tiwari R, Rai AK. Cyclodextrins in delivery systems: Applications. *J Pharm Bioall Sci*. 2010,2(2): 72-79.
- Wei Y, Zhang J, Zhou Y, Bei W, Li Y. Characterization of glabridin/hydroxypropyl- $\beta$ -cyclodextrin inclusion complex with robust solubility and enhanced bioactivity. *Carbohydr Polym*. 2017,159: 152-160.
- Xu XQ, Hong N, Zheng JW, Guo BB, Cheng L. Preparation of Aspirin- $\beta$ -Cyclodextrin Inclusion Complex by Grinding Method. *Adv Mater Res*. 2015,1120-1121: 882-885.
- Yamaguchi K. Evaluation of in-vitro and in-vivo antibacterial activity of tosufloxacin tosylate. *J Infect Chemother*. 2001,7(4): 205-217.
- Yoshida K, Kobayashi N, Saitoh H, Negishi T, Yamada T, Watanabe T, Kawakami S, Tari K, Satake I, Ozawa K. Clinical efficacy of tosufloxacin on the patients with urinary tract infections. *Hinyokika Kiyo*. 1992,38(1): 129.

Received for publication on 15<sup>th</sup> August 2018

Accepted for publication on 16<sup>th</sup> March 2020